

SHAKING TABLE TEST ON BEHAVIOR OF STEEL PIPE SHEET PILE FOUNDATION IN SLOPE DURING LIQUEFACTION

Nguyen Thanh TRUNG¹, Osamu KIYOMIYA², Tongxiang AN³ and Makoto YOSHIDA⁴

¹Student member of JSCE, Doctoral student, Waseda University (〒169-8555 Tokyo, Shinjuku-ku, Okubo 3-4-1)

²Fellow member of JSCE, Professor, Waseda University (〒169-8555 Tokyo, Shinjuku-ku, Okubo 3-4-1)

³Member of JSCE, A. Professor, Waseda University (〒169-8555 Tokyo, Shinjuku-ku, Okubo 3-4-1)

⁴Member of JSCE, Penta-Ocean Construction Co. Ltd. (〒329-2746 Nasushiobara, Shikuchou 1534-1 Tochigi)

1. INTRODUCTION

Many extensive damages to piles and other structures in areas of liquefaction has been observed in 1995 Hyogoken-nambu earthquake. Some of them are failures of piles near the bottom of liquefied layer and/or some cases are pile failures near the pile head. These failures are likely caused by the liquefaction due to decrease in the soil strength and/or the lateral movement of liquefied layer. Moreover, in the sites that located near or on revetment with a large sloping surface along river banks and sea coasts, there were some major damages observed at the both pile body and pile cap. This is likely caused by the unstable ground during the liquefaction. As the ground is in unstable state, seismic behavior of soil-pile foundation becomes complicated due to the change of physical properties of the ground and/or the ground motion. In recent years, many important lessons and insights regarding the basic mechanisms of soil-pile interaction in liquefied soil and their effect on superstructure performance during liquefaction have been learned from case histories, physical model tests, and numerical studies. However, most of these studies were conducted on the ground with a flat surface or with mild slope or near the water front line for pile foundation structure. Ramin Motamed *et al.*¹⁾ conducted large shaking table test on the pile foundation near a gravity-type quay with a flat ground. S. Mohsen Haeri *et al.*²⁾ and Ramin Motamed *et al.*³⁾ investigated the response of a group of piles to liquefaction-induced lateral spreading by large scale shake testing using a sloping ground of 5°. Tokida *et al.*⁴⁾ also conducted some sloping ground models of 5° with varying slope length, and Miyajima *et al.*⁵⁾

carried out the shaking table test and found that the response of pile depends on a sloping surface of ground with the sloping range was from 2° to 6°. Up to now, the effect of liquefaction in the revetment with a large ground slope has been little investigated.

Moreover, in the current bridge seismic design specification JRA *et al.*⁶⁾, the verification of seismic performance of foundation for liquefaction-induced lateral spreading is stipulated for the ground within a distance less than 100 m from a water front that formed by the revetment. Therefore, whether the foundation in the revetment is affected by liquefaction-induced lateral spreading or not is not clearly mentioned, and recommended that it is necessary to have further investigations and researches.

In this study, 1-G shaking table test with scale model 1:60 was designed for a testing model of steel pipe sheet pile foundation. The model is on the 15° slope ground named as a slope model. 2-D numerical modeling method was also conducted to investigate the behavior of steel sheet pile foundation comparing with test results. A total stress analysis (TDAP), a simpler method in engineering practice and the effective stress analysis (FLIP) were carried out and discussed in this study.

2. SHAKING TABLE TEST

The shaking table test was designed for the slope model to investigate their difference of behavior of the foundation subjected to liquefaction, as described in the following:

2.1 Soil container

The container has dimensions of 4 m length, 1.5 m

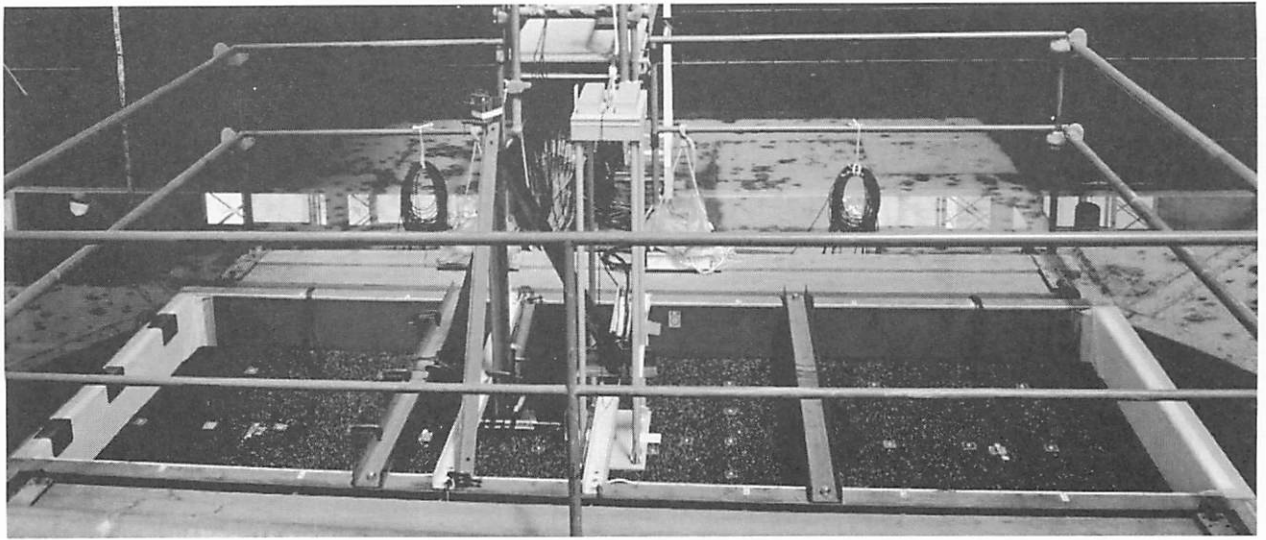


Fig.1 1-G shaking table test of a flat model.

width and 1.5 m height. It allows for free movement of soil along the transverse cross section and eliminates the influence of the friction between the container and the soil.

2.2. Physical model and material properties

In this study, all materials properties of physical model and ground were scaled using a similarity rule suggested by Iai *et al.*⁸⁾. Table 1 summarizes the scaling factors applied in this study.

Table 1. Scaling factors of shaking model test

Parameter	$\lambda = \text{prototype} / \text{model}$	Scale
Length	λ	60
Density	1	1
Time	$\lambda^{0.75}$	21.56
Stress	λ	60
Pore water pressure	λ	60
Displacement	$\lambda^{1.5}$	464.76
Acceleration	1	1
Strain	$\lambda^{0.5}$	7.75
Water permeability coefficient	$\lambda^{0.75}$	21.56
Bending stiffness	$\lambda^{4.5}$	100,387,728

The prototype of the model is a tower-steel pipe sheet pile foundation of a cable-stayed bridge that is planned in Tokyo Bay area. The foundation has 165 piles with dimension of 36.456 m length and 29.469 m width. Each pile has a diameter of 1500 mm and thickness of 25 mm.

The pier of physical model consists of four steel columns that rigid together by steel plate at the top with its mass of 60 kg. Each column has dimension of 1.1 m height and cross section in tubular shape of

2.27 cm diameter and 0.19 cm thickness. The foundation is a caisson made of acrylic material with dimension of 49 cm width, 60.8 cm length and 83.4cm height. The cap at the top of foundation is an acrylic plate with 60.8 cm length, 49 cm width and 98 cm thickness. The footing of pier was made of steel with dimensions of 26.6 cm length, 46.6 cm and 18.5 cm thickness. Detail of physical models is shown in the Fig. 3.

The ground in the models consisted of a 48.8 cm liquefiable sand layer with a relative density of 50 % overlying a 74.3 cm non-liquefiable with a relative density of 90 % using Yamagata-sand No. 6 (D50 = 0.3 mm) and the rubble layer used Grade 6 crushed stone with a particle size of 13-20 mm. The grain size distribution of Yamagata sand used for the ground is shown in Fig.2. The slope of ground was 15° in longitudinal direction. Waterfront level in both models is approximately considered at the ground surface.

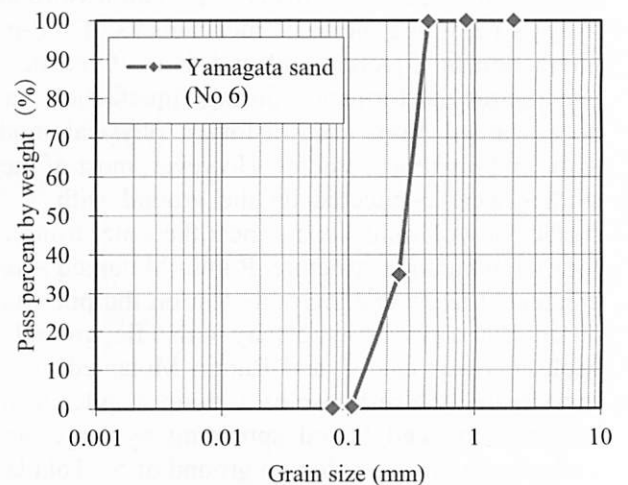


Fig.2 Grain size distribution of Yamagata sand

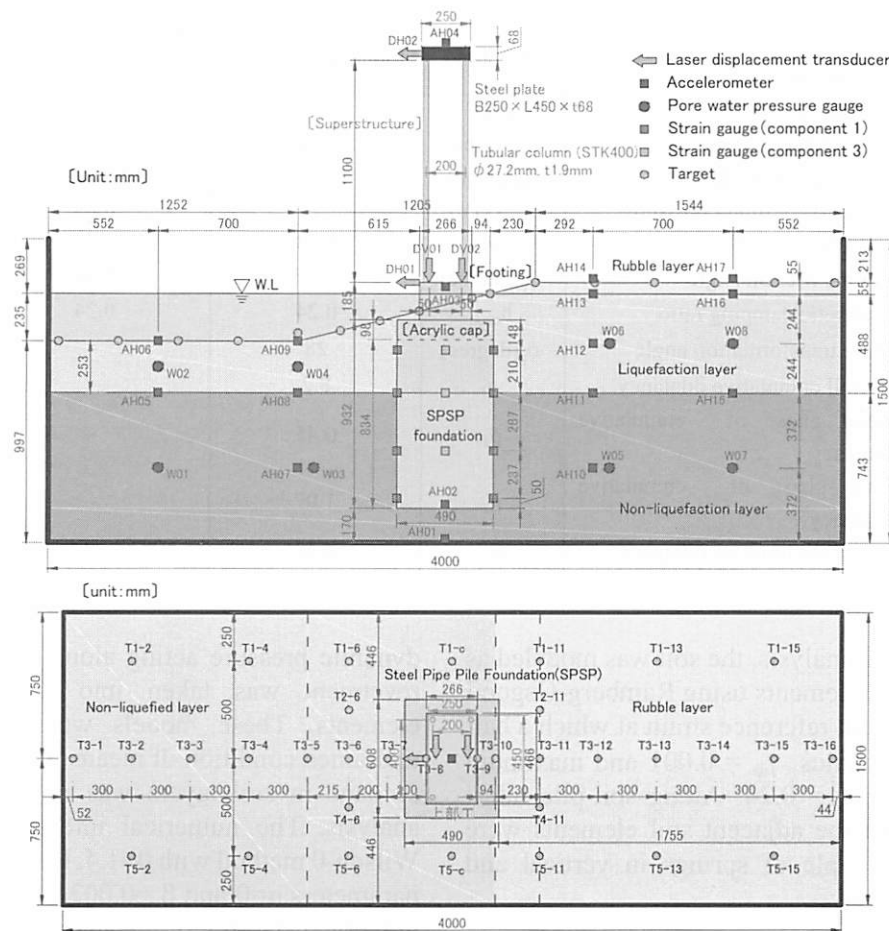


Fig.3 General view of a slope model.

2.3. Instrument and arrangement

The instruments and their arrangement are shown in Fig.3. The accelerometers and pore pressure transducers were arranged in area of near field and far field of ground at various depths of liquefied layer and non-liquefied layer. The accelerometers were attached at the top and bottom of the pier. There were two horizontal laser displacement transducers at the top and the bottom of the pier and two vertical displacement transducers were at the bottom of the pier. The strain gauges were installed on opposite sides of the foundation at different depths to record bending strains. The targets were pasted on the ground surface to record its movement after shaking.

2.4. Base excitation

The models were shaken with base harmonic acceleration with a constant frequency of 10 Hz with duration time is 2 s. Its amplitude increased step by step, one of input waves is shown in Fig.4.

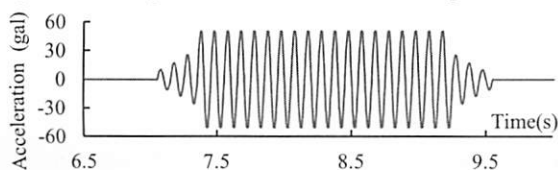


Fig.4 Acceleration wave input at the base.

III. NUMERICAL ANALYSIS

In this study, 2-D finite element model was used to simulate for a slope model of shaking table test following two kinds of analyses considered liquefaction conditions. The first was a total stress analysis (TSA) using reduction factor for shear modulus of soil stipulated in JRA *et al.*⁽¹⁾. TDAP III program was available in this analysis. The second was an effective stress analysis (ESA) and was employed by a strain space multiple shear mechanism model, called Multi-Spring Model. FLIP program was available in this analysis.

3.1 Total stress analysis

The nonlinear dynamic analysis was conducted by a time history direct integration method on these models. The boundary at the bottom of model was fixed in the vertical and horizontal direction and lateral boundary at the two sides of model was fixed in the horizontal direction. The piles, pier columns and acrylic plate at the top of pier were modeled as elastic beam elements. The steel footing plate and the acrylic cap of piles were modeled as elastic strain plane elements.

Table 2. List of soil parameters

Parameter		Symbol	Liquefaction layer	Non-Liquefaction layer	Rubble layer
Parameters for deformation characteristics	Wet unit weight	ρ (t/m ³)	1.96	2.05	1.37
	Initial shear modulus	G_{ma} (Kpa)	3,866	21,788	2,993
	Initial bulk modulus	K_{ma} (Kpa)	10,083	56,819	7,805
	Standard confining pressure	σ_{ma}' (kPa)	2.27	6.85	0.28
	Poisson's ratio	ν	0.33	0.33	0.33
	Internal friction angle	ϕ_f (degree)	36.55	42.80	41.60
	Hysteretic damping ratio	h_{max}	0.24	0.24	0.24
	Phase transformation angle	ϕ_p (degree)	28	-	-
Parameters for dilatancy characteristics	Overall cumulative dilatancy	w_l	8.2	-	-
	Initial phase of cumulative dilatancy	p_1	0.45	-	-
	Final phase of cumulative dilatancy	p_2	1.07	-	-
	Threshold limit for dilatancy	c_1	4.48	-	-
	Ultimate limit of dilatancy	S_1	0.005	-	-

In the total stress analysis, the soil was modeled as plastic strain plane elements using Ramberg-Osgood model with the initial reference strain at which a half of initial shear modulus, $\gamma_{r0} = 0.001$ and maximum damping factor, $h_{max} = 0.24$. Along soil-pile interface, the piles and the adjacent soil elements were connected by a couple of springs in vertical and horizontal directions.

3.2. Effective stress analysis

In the effective stress analysis the boundary conditions were same as those of the total stress analysis. The piles, pier columns and the plate were also modeled as elastic beam elements and the footing and pile cap were modeled as elastic strain plane elements.

The soil was considered as strain plain elements using a Multi-Spring model with the parameters for deformation and for dilatancy characteristic of soil layers that are summarized in Table 2. The hydro-

dynamic pressure acting along slope surface of the revetment was taken into account using fluid elements. These models were calculated in the undrained condition. It means that the effect of water seepage in soil layers was not considered in this analysis. The numerical integration was done by Wilson- θ method with $\theta=1.4$. Reyleigh damping with parameters $\alpha=0$ and $\beta=0.002$ was adopted to ensure numerical stability of the analysis.

In both the analyses, the self-weight analysis step was firstly conducted to calculate the initial stress and strain of the model before a dynamic analysis step.

IV. RESULTS AND DISCUSSION

4.1. Result and comparison between the total and the experiment

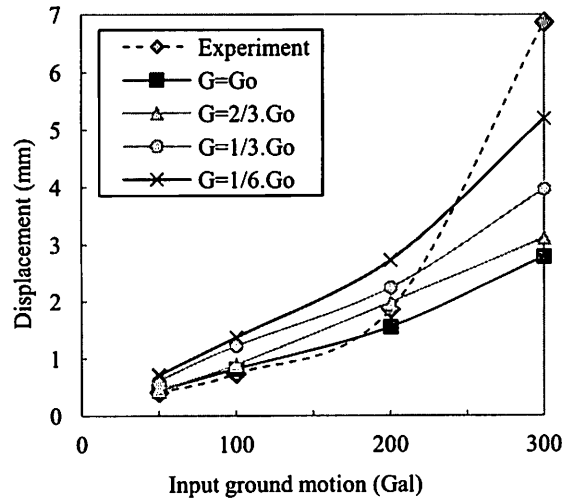


Fig. 5 Displacement of superstructure in a slope mode I in the total stress analysis

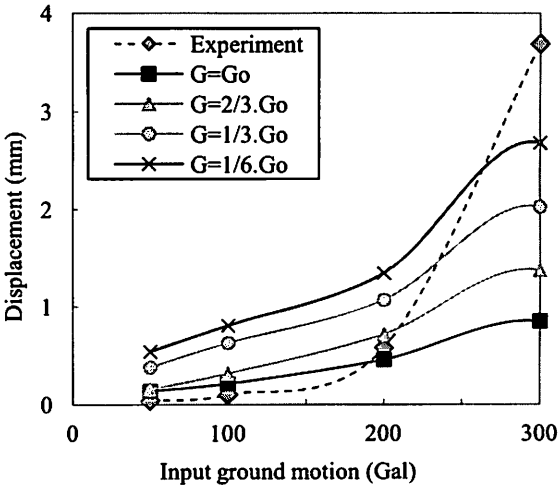


Fig.6 Displacement of pile cap in a slope model in the total stress analysis

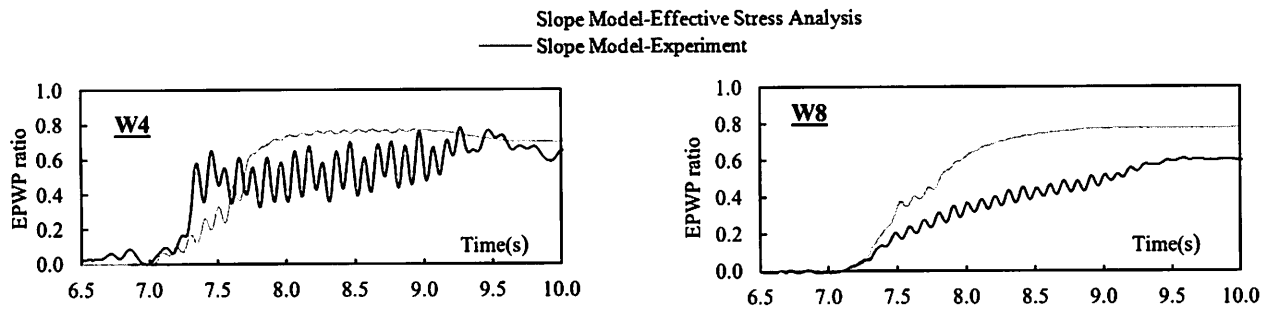


Fig.7 Excess pore water pressure at W4 and W8 in the slope model under 300 gal input ground motion.

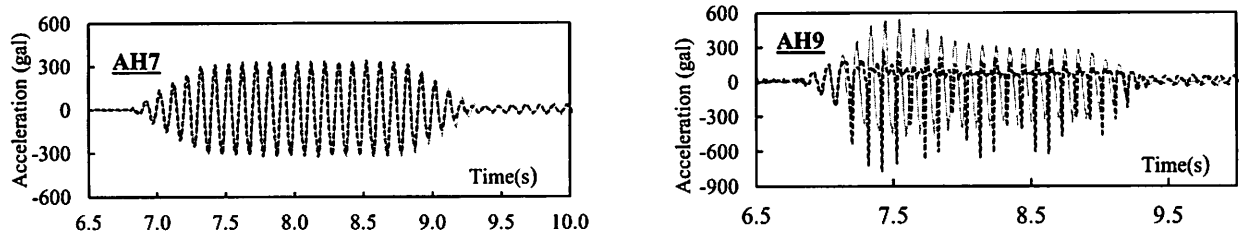


Fig.8 Acceleration at AH7, AH9 in the slope model under 300 gal input ground motion.

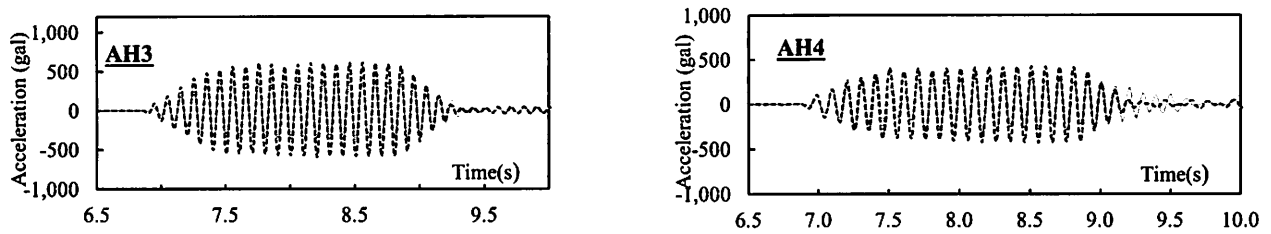


Fig.9 Acceleration response of superstructure and pile cap in a slope model under 300 gal

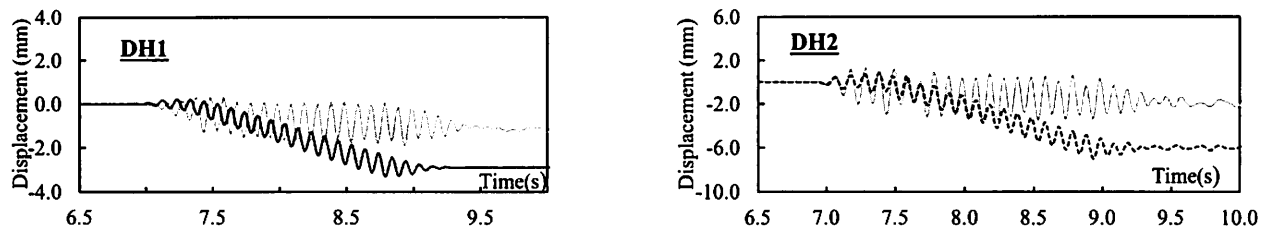


Fig.10 Horizontal displacement response of superstructure and pile cap in a slope model under 300 gal

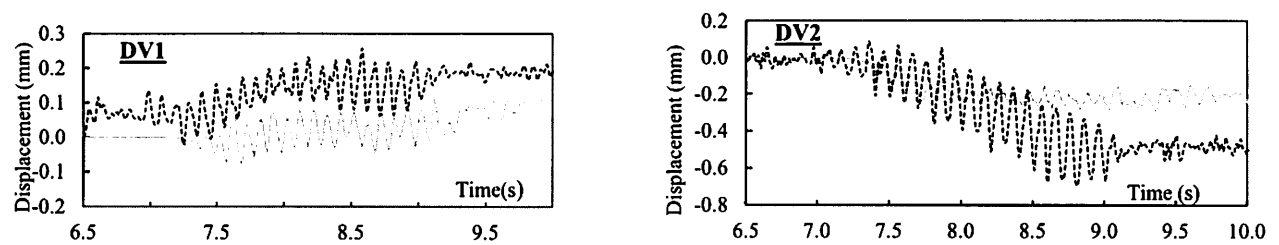


Fig.11 Vertical displacement response of superstructure and pile cap in a slope model under 300 gal

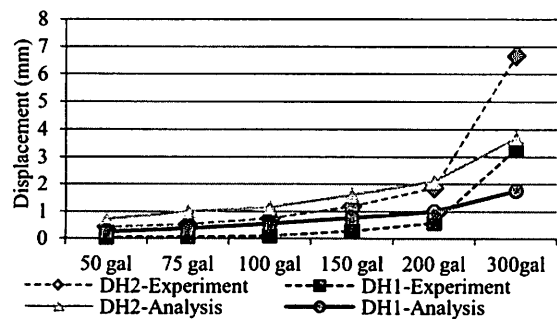


Fig.12 The maximum displacement at DH1 and DH 2 from 50 gal to 300 gal

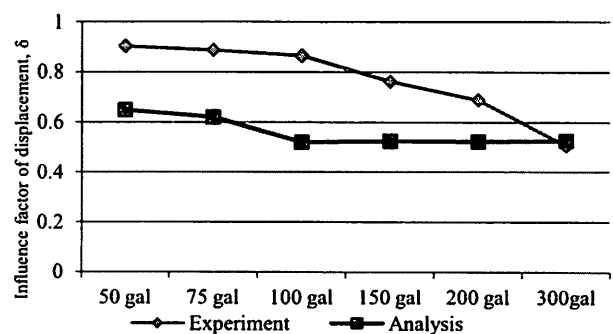


Fig.13 Influence factor of displacement

This analysis was carried out by gradually reducing the shear modulus of the liquefaction layer G_0 , $2/3G_0$, $1/3G_0$ and $1/6G_0$. The maximum horizontal response displacement at the superstructure and the pile cap in the slope model considering the reduced shear modulus are shown in Fig.5 and Fig.6. The residual displacement is not calculated in the total stress analysis. Here the maximum response displacements are argued.

Fig.5 and Fig.6 illustrates that in the slope model the maximum response displacement of the superstructure and the pile cap in the experiment resembles that in TSA in case of the original shear modulus G_0 . Next, from 150 gal to 200 gal the displacement of the experiment was within the range of the displacement between $2/3G_0$ and $1/3G_0$ case in TSA. Finally, in case of 300 gal the displacement of the experiment was over the maximum displacement of $1/6G_0$ case. The result indicates that in case of the high amplitude input ground motion TSA method may not produce the natural response of the slope model. This may be because there was instability of the slope ground. It means that the liquefaction phenomenon with a reduction of soil strength and lateral spreading occurred at the same time.

4.2 Result and comparison between the effective

stress analysis and the experiment

a) Behavior of ground

The excess pore water pressure at W4 and W8 point under 300gal input ground motion are shown in Fig.7 and the horizontal acceleration at AH7, AH9 are shown in Fig.8. It is seen that both the peak of EPWP ratio at the near field W4 and far field W8 of the effective stress analysis (ESA) were higher than these of the experiment. In the non-liquefaction layer the acceleration at AH7 of ESA had a good agreement with that of the experiment and there was not any amplitude variations of the acceleration during shaking time. Meanwhile, the acceleration at near field AH9 of the liquefaction layer had a significant variation which started at the time of 7.5s and these amplitude gradually reduced from the time of 7.5s to the time fo 10s. It means that the generation of the pore water pressure increased with the loss of soil strength, clearly this made the decrease of the acceleration amplitude in liquefaction layer. Moreover, the Fig.8 shows that at AH9 the negative acceleration that has the direction from the water ward to the land ward, took advantage and its amplitude became larger than that of the positive acceleration. It thinks that because the instability of the slope ground which occurred very fast in the

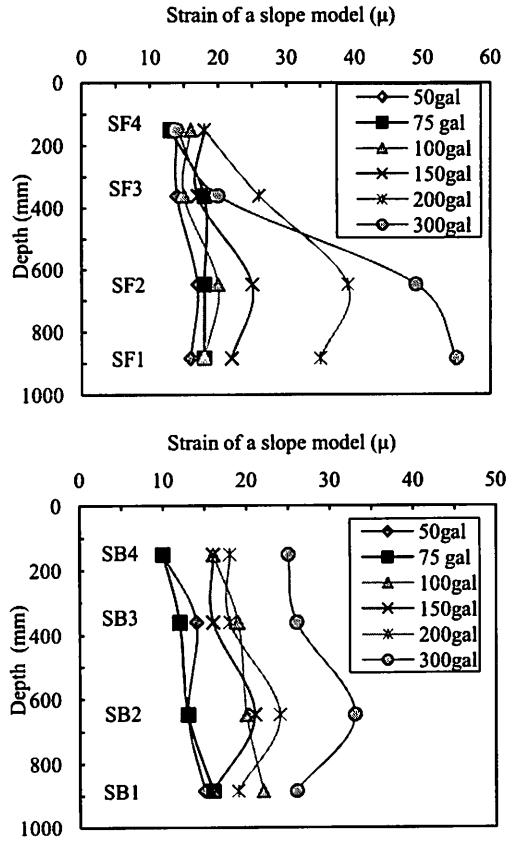


Fig.14 Strain distribution of the experiment in the front side and the back side in the slope model.

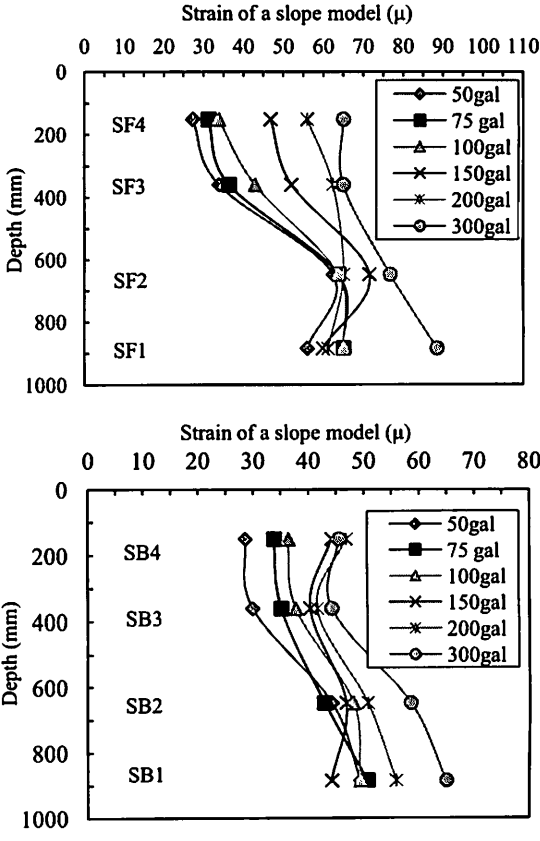


Fig.15 Strain distribution of effective stress analysis in the front side and the back side in the slope model.

direction from the land ward to the water ward generated the high acceleration. As a result, this made the advantage of negative acceleration.

b) Behavior of the superstructure and pile cap

The horizontal acceleration response of the superstructure and pile cap of the slope model under 300 gal input ground motion are shown in Fig.9. Both the acceleration of the superstructure and the pile cap of the experiment was larger than these of ESA. The horizontal and vertical displacement of the pile cap and superstructure under 300gal in the slope model are shown in Fig.10 and Fig.11. It is seen that the residual displacement appeared in ESA and the difference of the maximum displacement between ESA and the experiment was quite large. The result of vertical displacement indicates that the experiment and ESA had the same trend is that the point DV1 subsided in the downslope direction, while the point DV2 rise in the upslope direction.

The Fig.12 shows the horizontal displacement at the superstructure DH2 and at the pile cap DH1 from 50 gal to 300 gal input ground motion for both the experiment and effective stress analysis. This figure shows that from 50 gal to 200 gal their displacement gradually increased but in case of 300 gal the displacement sharply increased. Both the experiment and effective stress analysis have the same trend. It thinks that the slope ground was unstable and produces the lateral spreading pressure.

To express the behavior of foundation and the superstructure on foundation, the influence factor δ was calculated as the below equation:

$$\delta = \frac{\text{Response of DH2} - \text{Response of DH1}}{\text{Response of DH2}} \quad (1)$$

The influence factor result is shown in Fig.13. This figure shows that both the experiment and the effective stress analysis have the same trend is that that from 50 gal to 100 gal, the difference of the displacement and acceleration between DH1 and DH2 was significant, however in cases from 100 gal to 300 gal the difference gradually became smaller. Especially, in case of 300 gal the difference was sharply decreased. It means that the under high amplitude input ground motion the effect of movement of the slope ground is really significant. The kinematic force took advantage.

c) Behavior of the foundation

The maximum strain distribution of the experiment along the front side (SF) and the back side (SB) of the foundation in the slope model from 50 gal to 300 gal are shown in Fig.14. The strains of the effective stress analysis are shown in Fig.15.

Generally, the strain in both the experiment and

ESA almost reaches a maximum value near the bottom of pile foundation such as at SF2, SB2 or SF1, SB1, and the maximum strain was obtained at SF1 on the front side in a slope model. However, in cases from 100 to 300 gal the difference became significantly larger. It means that the strain on the front side was larger than that on the back side and the distribution of the strain was asymmetric. Moreover, the maximum strains in ESA were almost larger than those in the experiment.

CONCLUSIONS

The shaking table test and numerical analysis were conducted on steel sheet pipe pile foundation in the slope to investigate the dynamic behavior for liquefaction. Based on the results, there are main findings as follows:

- 1) There is fairly good agreement as to pore water pressures and accelerations between the experiment and effective stress analysis. In case of 300 gal input ground motion, the residual displacement values of the superstructure and pile cap increased when liquefaction of sand occurred. The effective stress analysis gave conservative result for the test result.
- 2) The response displacement by the total stress analysis using a reduction of soil strength stipulated in JRA 2002 does not have a good agreement with the experiment when input acceleration is large and liquefaction occurs. In the slope model under the high amplitude input ground motion, the lateral spreading of the liquefaction layer occurs.

REFERENCES

- 1) Matsui, T., Kitazawa, M., Nanjo, A. and Yasuda, F.: Investigation of damaged foundations in the Great Hanshin earthquake disaster. *Seismic Behavior of Ground and Geotechnical Structures*, Secoe Pinto (ed.), Balkema, Rotterdam, 235-242. *Geotechnical Engineering (KIG – Forum 97)*, Kansai Branch, Japanese Geotechnical Society, Osaka, Japan, 1997.
- 2) Ramin, M., Towhata, I., Honda, T., Tabata, K. and Abe, A.: Pile group response to liquefaction-induced lateral spreading: E-Defence large shake table test. *Journal Soil Dynamics and Earthquake Engineering*, Vol. 51, pp.35-46, 2013
- 3) Haeri, S.M., Kavand, A., Rahmani, I., Torabi, H.: Response of a group of piles to liquefaction-induced lateral spreading by large scale shaking testing. *Journal of Soil Dynamic and Earthquake Engineering*. Vol. 38, pp.25-45, 2012.
- 4) Motamed, R., Sesove, V., and Towhata, I.: Shaking model test on behavior of group piles undergoing lateral follow of liquefied subsoil. *Proc. 14th Word Conference on Earthquake Engineering*. Beijing, China, pp.12-17, 2008.
- 5) Tokida, K., Matsumota, H., & Iwasaki, H.: Experimental study on drag acting on piles in ground flow-

- ing by soil liquefaction. *Proc. 4th US-Japan Workshop on Earthquake Resistant Design of Lifeline Facilities and Countermeasures for Soil Liquefaction*, NCEER report 92- 0019, SUNY, Buffalo, pp.511-523, 1992.
- 6) Miyajima M, Kitaura M, Ando K.: Experiments on liquefaction-induced large ground deformation. *Proceedings of the third Japan-U.S. workshop on earthquake resistant design of lifeline facilities and countermeasures for soil liquefaction*, Technical report NCEER, New York: SUNY, Vol. 1, pp. 269-78, 1991.
 - 7) JRA: Specifications for highway bridges. Japan Road Association, Preliminary English Version, prepared by Public Works Research Institute (PWRI) and Civil Engineering Research Laboratory (CRL), Japan, November, 2002.
 - 8) Iai, S.: Similitude for Shaking Table Tests on Soil-Structure Model in 1G Gravitational Field. *Report of the Port and Harbor Res.Inst.* Vol.27, No.3, pp.3-24, 1988.